Bright High-Order Harmonic Generation From Long Gas Jets Toward Coherent Soft X-Ray Applications

H. T. Kim, I. J. Kim, V. Tosa, C. M. Kim, J. J. Park, Y. S. Lee, A. Bartnik, H. Fiedorowicz, and C. H. Nam

***Abstract*—We have performed the optimization of high-order harmonic brightness from long gas jets by using self-guided and chirped femtosecond laser pulses and analyzed their coherence properties. The characteristics of laser pulse propagation were analyzed both in theory and in experiments to understand the self-guiding process of laser pulses and chirp compensation mechanism. Highly efficient harmonic generation with low beam divergence and narrow bandwidth was achieved by applying these two techniques to the long gas jets. The coherence properties of the bright harmonics were examined using double-pinhole interference and spectral interference.**

***Index Terms*—Extreme ultraviolet (EUV) interferometry, femtosecond laser, high-order harmonics, optical field ionization.**

I. Introduction

HIGH-ORDER harmonics are generated in the extreme ultraviolet (EUV)/soft X-ray region by an interaction of atoms with an intense femtosecond laser field. High-order harmonics have attracted much attention due to their unique properties such as excellent coherence [1], [2], wavelength tunability [3], [25] ultrashort duration [4], and tabletop scale. Rapid advances in the development of intense femtosecond lasers have prompted equally rapid progress in high-order harmonic generation research. Intense femtosecond laser pulses have been used to generate high-order harmonics in the water window region [5], which is important for biological applications. Experimentally achieved harmonic generation efficiencies have reached the limit set by the gas absorption [6]. In addition, absolute phase-locked laser pulses have opened a way to generate a single burst of attosecond EUV pulse from high-order harmonics [7]. Thus, over the past decade, high-order harmonic generation has been one of the most intensively pursued subjects in the area of high-field physics.

A significant enhancement of harmonic brightness is needed to facilitate practical applications. Constant *et al.* [8] reported on the concept of absorption-limited harmonic generation within the framework of static and one-dimensional (1-D) phase matching. Recent efforts in this area have extended such studies to include optimal phase-matching conditions in time and three-dimensional (3-D) space for obtaining higher efficiency. Kazamias *et al.* [9] reported a time-dependent phase-matching analysis, wherein the maximum atomic response is made to occur at the time of good phase matching. In spatial domain, self-guided laser pulses produce bright harmonics due to the reduction of plasma defocusing effects and accomplishment of uniform phase matching of harmonics in the radial and axial directions [10]–[12]. The coherent control of high-order harmonic generation using chirped laser pulses [13], [14] was also applied to control the spectral structure of harmonics. By this technique, the spectral bandwidth of the harmonics can be tailored to suit specific applications such as the one requiring a narrow spectrum for interferometry or a quasi-continuous spectrum for EUV absorption spectroscopy. Applications of high-order harmonics, such as interferometry and holography, demand a high degree of coherence of the harmonics in addition to the high brightness. We have previously reported spatial-coherence measurements for harmonics from Ar by using double-pinhole interference, which showed almost perfect coherence over nearly entire harmonic beam cross section [2]. This result has opened the way to apply harmonics to point-diffraction interferometry and EUV metrology. In the temporal domain, Salieres *et al.* [15] demonstrated spectral interferometry with high-order harmonics. Their results showed that two phase-locked harmonic sources, delayed in time, can be generated by using two temporally separated laser pulses. Therefore, the harmonics are becoming very useful coherent EUV/soft X-ray sources.

In this paper, we have demonstrated bright harmonic generation from long gas jets using self-guided and chirped laser pulses. The long gas jet was selected for bright harmonic generation due to the simplicity in target alignment and the capability of coupling large laser energy into a large interaction volume. To utilize this long and dense medium for bright harmonic generation, the evolution of laser pulses in the ionizing medium should be understood in both the space and time domains. For a proper understanding of self-guiding and laser chirp control, we have analyzed, both experimentally and theoretically, the propagation characteristics of laser pulses in an ionizing medium and obtained the conditions for self-guided propagation and laser chirp control. With self-guided negatively chirped laser pulses, a bright 61st harmonic at 13 nm was generated with low beam divergence of 0.5 mrad and a narrow bandwidth of 0.07 nm. We

Manuscript received March 25, 2004; revised September 15, 2004. This work was supported by the Ministry of Science and Technology of Korea through the Creative Research Initiative Program.

H. T. Kim, I. J. Kim, C. M. Kim, J. J. Park, Y. S. Lee, and C. H. Nam are with the Department of Physics, Korea Advanced Institute of Science and Technology (KAIST), Daejeon 305-701, Korea (e-mail: htkim@kaist.ac.kr).

V. Tosa is with the National Institute for Research and Development in Isotopic and Molecular Technologies (NIRDIMT), Donath 69-103, Cluj-Napoca, Romania.

A. Bartnik and H. Fiedorowicz are with the Institute of Optoelectronics, Military University of Technology, Warsaw 00-908, Poland.

Digital Object Identifier 10.1109/JSTQE.2004.837739

have summarized the conditions for bright harmonic generation from a long jet of noble gases. For the certification of coherence, we performed two kinds of interference experiments with high-order harmonics: double-pinhole interference and spectral interference.

This paper is organized as follows. The analysis on laser propagation in ionizing medium is described in Section II and results of bright harmonic generation are presented in Section III. The interference experiments with high-order harmonics are described in Section IV. The summary is given in Section V.

II. Laser Propagation in an Ionizing Gas Medium

Spatial and temporal characteristics of a laser pulse propagating through an ionizing gas medium can be affected by the refractive index modulation that may vary in time and space. In space domain, a Gaussian beam (or any peaked laser beam) produces a higher electron concentration in its central part than in the outer region, which results in the defocusing of the laser field [16]. On the other hand, the refractive index modulation induced by a variation of electron density in time induces the self-phase modulation (SPM) of the laser pulse [17]. Since these two effects can substantially modify the pulse characteristics, control of the ionization effects is an important issue in the investigation of the interactions between atoms and intense femtosecond laser pulses, such as high-order harmonics, self-channeling in air, and laser-assisted particle acceleration.

To investigate the laser pulse propagation in an ionizing medium, we performed 3-D simulations of laser pulse propagation [10]. In an ionizing medium, the pulse propagation is affected by diffraction, refraction, nonlinear self-focusing, ionization, and plasma defocusing. The pulse evolutions in such media are described by the wave equation which can be written as

$$\nabla^2 E_1(r,z,t) - \frac{1}{c^2}\frac{\partial^2 E_1(r,z,t)}{\partial t^2} = \frac{\omega^2}{c^2}(1-\eta_{\text{eff}}^2)E_1(r,z,t) \tag{1}$$

where $E_1(r,z,t)$ is the transverse electric field of the laser with frequency ω. Since radial symmetry is assumed, cylindrical coordinates are used throughout the simulation. The effective refractive index of the medium can be written as $\eta_{\text{eff}}(r,z,t) = \eta_0 + \eta_2 I(r,z,t) - \omega_p^2(r,z,t)/2\omega^2$. The first linear term $\eta_0 = 1 + \delta_1 + i\beta_1$ accounts for the refraction (δ_1) and absorption (β_1), while the second term describes a $\chi^{(3)}$ process depending on laser intensity I, which is well known as the optical Kerr effect. Finally, the third term reflects the generated electron effects on laser pulse propagation, which contains the plasma frequency $\omega_p = (4\pi e^2 n_e/m)^{1/2}$ and accounts for the presence of a density n_e of electrons per unit volume. m and e are mass and charge of electron, respectively.

The spatial and temporal changes of the laser profile during propagation were carried out for the case of a negatively chirped 42-fs pulse with 5-mJ energy. The gas medium was a 9-mm Ne gas jet with a density of 1.4×10^{18} cm^{-3}. The reason for using a negatively chirped pulse is to control the SPM effect and will be discussed later in detail. Truncated Gaussian pulses, which were focused with a power of f/85, were used in the calculation to closely follow actual experimental conditions. The gas jet position is defined as z = 0, when the center of the gas jet is positioned at the laser focus. Fig. 1 shows the evolution of laser beam profiles at the time of pulse peak along the laser propagation at the two gas jet positions of z = 0 and z = −18 mm. The negative sign means that the gas jet is located before the laser focus. At z = 0 [Fig. 1(a)], the laser beam spreads quickly due to plasma defocusing. After the propagation, the laser intensity decreases to 3×10^{14} W/cm^2, while the initial intensity is more than 1×10^{15} W/cm^2. However, when the gas medium is placed 18 mm before the laser focus, the laser beam forms a flattened profile while keeping similar peak intensity with the initial laser pulse.

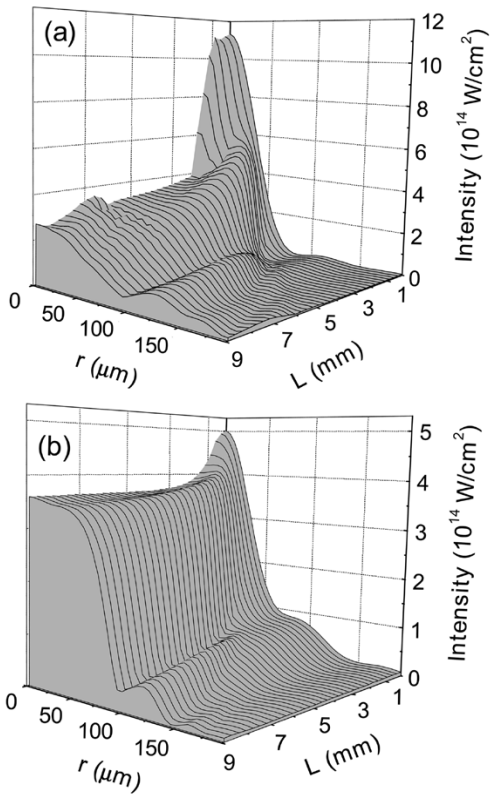

Fig. 1. Evolution of the laser beam profile in an ionizing medium calculated by 3-D simulation. L is the propagation distance measured from the entrance plane of a 9-mm gas jet. Gas jet positions are: (a) z = 0 and (b) z = −18 mm.

The profile flattening and guiding of the laser pulse, when the gas jet is placed before the laser focus, arises due to the balance between plasma defocusing and the convergence of the focused laser beam. When the gas jet is positioned before the laser focus, the central part of laser beam is refracted outward by the electron density gradient, while the less affected outer part continues to converge. This behavior of the laser pulse in the ionizing medium creates the flattened profile. After the formation of the flattened profile, the electron density is also flattened in the same region but rapidly drops at the boundary. This rapid change of the electron density results in a sharp refractive index change at the boundary and, thereby, a wave-guide is created. Therefore, the profile flattening and self-guiding of laser pulses can be achieved by choosing a proper gas jet position [12].

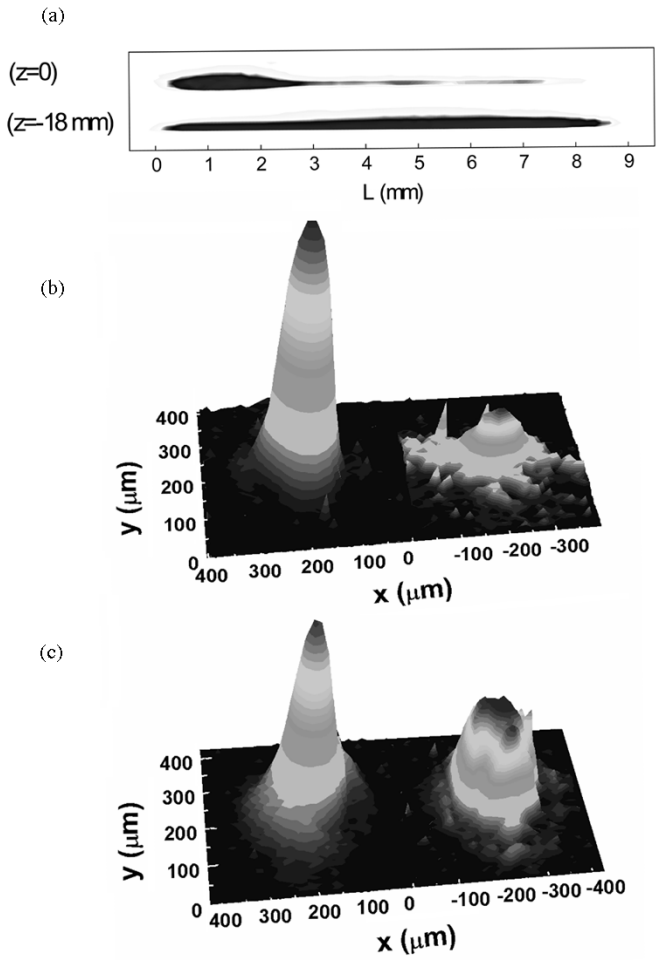

Fig. 2. (a) Visible images of Ne plasma obtained at two gas jet positions $z = 0$ and -18 mm. Laser beam profiles at the entrance (left) and exit (right) of the gas jet for the cases of (b) $z = 0$, and (c) $z = -18$ mm.

To experimentally confirm the self-guided propagation and profile flattening of laser pulses, we captured visible plasma images along the propagation direction and radial profiles of the laser beam at the exit of the medium using charge-coupled device (CCD) detectors. The experiments were performed using chirped femtosecond laser pulses from a chirped pulse amplification (CPA) Ti:sapphire laser operating at 10-Hz repetition rate [18]. The visible plasma images were captured from a transverse direction and the laser beam profile at the end of medium was obtained by imaging it on a CCD. The same conditions as those for the 3-D calculations were used in the experiments. The visible plasma image changed drastically with gas jet positions. At the gas jet position of $z = 0$ [Fig. 2(a)], the plasma image was bright only for the first 2-mm section of the medium. It is in good agreement with the 3-D calculation which showed the rapid decrease of laser intensity in the first 2 mm due to plasma defocusing. As the gas jet position moved away from the laser focus, the bright part of plasma image was extended and a nearly uniform plasma image over the entire gas jet was formed at $z = -18$ mm. This also matched the 3-D calculation result very well, which shows that self-guiding occurs for $z = -18$ mm, as shown in Fig. 1(b).

The laser beam profile at the end of the medium can be direct evidence of the profile flattening. Fig. 1(b) and (c) shows the laser profiles at the gas jet positions $z = 0$ and $z = -18$ mm. At $z = 0$, the laser profile was severely distorted and weakened after the propagation. On the other hand, at $z = -18$ mm, the laser beam formed a flattened profile with a radius of 60 μm, which closely matched the 3-D calculation. It is thus clear that a proper selection of the gas jet position is critical for the profile flattening and self-guiding of laser pulses.

Next, we analyzed the SPM effects on pulse propagation by a time-frequency analysis using the spectrogram method [19], [20]. A distribution function in the time-frequency domain is a powerful tool to analyze an electric field with a time-dependent frequency distribution, which cannot be revealed by an ordinary Fourier transform method. The temporal evolution of a laser field on axis was calculated by 3-D simulation with same parameters as used in Fig. 1(b). Fig. 3 shows the change of laser chirp structure during the pulse propagation. The solid circles show the contour of the Wigner distribution function and the dotted lines indicate the mean frequency at a given time. It clearly shows the temporal modification of laser chirp structure caused by SPM. After 1-mm propagation, the initial negative chirp was modified by the SPM and laser pulses became nearly chirp-free in the leading edge. This positive chirp in the leading edge of the laser pulse increased with the propagation length and it overcame the initial negative chirp after 4-mm propagation.

We applied negatively chirped pulses to control the effect of SPM in the leading edge. Since the high-order harmonics are generated coherently by a driving field, this frequency modulation of laser pulse directly affects the spectral structure of the harmonics. To generate sharp and bright harmonics, the initial chirp of laser pulses can be chosen to compensate for SPM-induced laser chirp at the instant of harmonic generation. In the case of chirp-free or positively chirped laser pulse, SPM-induced positive chirp in the leading edge of the laser pulse can be severe enough to broaden the generated harmonic spectrum as the phase-matched harmonics are mainly generated in the leading edge. When we use negatively chirped pulses, the induced positive chirp in the leading edge can be reduced and matched with dynamically induced negative chirp of harmonics, which results in generating sharp and bright harmonics.

In this section, we have discussed techniques to control the spatial and temporal profiles of intense femtosecond laser pulses; one is the profile flattening and self-guiding of a laser pulse achieved by properly selecting a gas jet position, and the other is the control of SPM effects by using an appropriately chirped laser pulse. These two techniques can be simultaneously applied for the generation of bright high-order harmonics, which should, in turn, lead to the spatiotemporal control of high-order harmonic generation.

III. Bright High-Order Harmonic Generation by Tailoring a Laser Pulse

High-order harmonic generation is intrinsically related to the ionization of gas medium because it accompanies an ionization process in an intense laser field. In the case of a long and high-density medium, the modification of the spatiotemporal

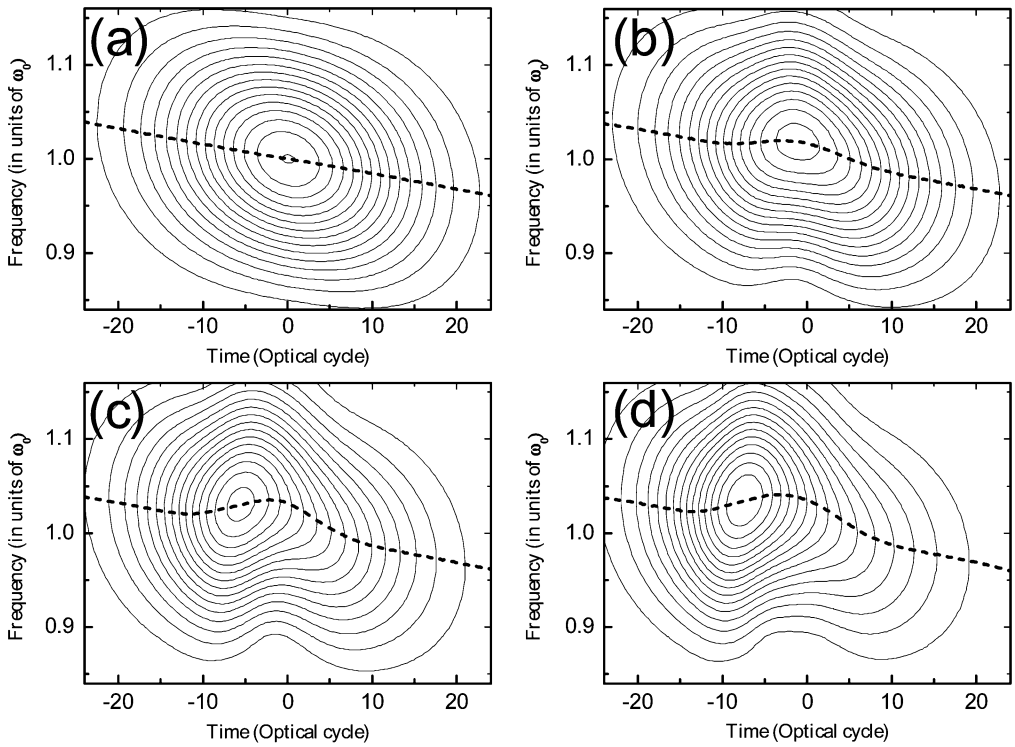

Fig. 3. Spectrograms of a propagating laser pulse through a 9-mm Ne medium with propagation length of (a) $L = 0$, (b) $L = 1$ mm, (c) $L = 4$ mm, and (d) $L = 9$ mm.

structure of the laser pulse itself by the ionizing medium should be taken into account since it is closely linked with the harmonic efficiency and spectral structure. In this section, we describe the generation of bright harmonics with narrow spectral bandwidth using profile-flattened and chirp-controlled femtosecond laser pulses interacting with a long gas jet.

We have investigated high-order harmonic generation using a 9-mm long Ne gas jet in the wavelength region of 10.0–18.0 nm. The harmonics were detected by a flat-field EUV spectrometer equipped with a back-illuminated X-ray CCD [21] and the scattered laser light was blocked by two 200-nm Zr filters. Fig. 4(a) shows the harmonic spectra obtained at several gas jet positions with negatively chirped 42-fs laser pulses. The harmonic spectra showed a strong dependence on the gas jet position, which is directly linked to the drastic change of laser propagation characteristics with gas jet position. At the gas jet positions $z = 0$ and $z = +8$ mm, the harmonics in the 13-nm region were much weaker than in other cases, because the plasma defocusing severely decreased the effective interaction volume for harmonic generation. As the gas jet position was shifted away from laser focus, the harmonic signal greatly increased and was maximum at $z = -18$ mm, where the self-guiding and profile flattening occurred as shown in Fig. 2.

The 61st harmonic, at the wavelength of 13.4 nm, was the strongest harmonic at $z = -18$ mm. While the higher orders were diminished as they were in the cutoff region, the lower orders were weak due to strong gas absorption. Since the medium length with this gas density corresponds to six times the absorption length in Ne, the generated harmonics are limited mainly by the absorption in Ne. At this optimum condition, the 61st harmonic was strong enough to saturate the X-ray CCD with one laser shot of 5 mJ. We performed the energy calibration of the 61st harmonic by inserting an EUV silicon photo diode (International Radiation Detectors AXUV-100) at the same place as the X-ray CCD. The energy of the optimized 61st harmonic was estimated to be 0.4 nJ by assuming nominal values for the diffraction efficiency of the grazing incidence flat-field grating, reflectance of toroidal mirror, transmission of Zr filter, and quantum efficiency of EUV silicon diode. This is a very conservative value because the oxidation and contamination of optics in spectrometer and silicon detector with time were not taken into account.

A good phase matching between generated harmonics and a driving laser pulse can be achieved by setting up the self-guided and profile-flattened laser pulses. Once the profile flattening and self-guiding of laser pulses is established, the geometric phase and the atomic phase do not contribute appreciably to the phase matching conditions due to the collimated propagation and uniform intensity distribution of the laser pulses. In this case, the dispersion by neutral atoms and free electrons mainly determines the phase matching conditions. Just considering the dispersion, the 61st harmonic from neon atoms satisfies the phase matching conditions at the ionization level of about 1%. In the 3-D simulation, we observed that this ionization level occurred at the leading edge of the laser pulse after the profile flattening was developed. The profile flattened and self-guided laser pulses provide uniform phase-matching conditions over a large cross section by overcoming the problems associated

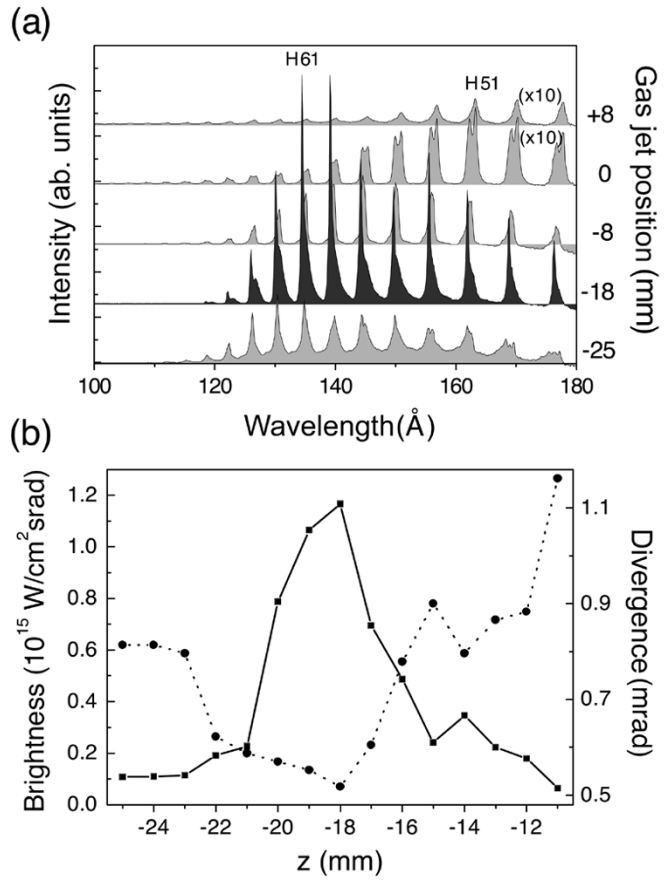

Fig. 4. (a) Harmonic spectra at different gas jet positions. First two spectra are multiplied by 10. "Hn" denotes nth order harmonic. (b) Divergence (solid circles) and brightness (solid square) of 61st harmonic.

with the variation of phase-matching conditions along the radial direction [10]. Therefore, the self-guiding and profile flattening provided an ideal condition for well phase-matched strong harmonic generation in a large volume.

We measured the divergence of the harmonics by installing a cylindrical mirror instead of the toroidal mirror in the flat-field EUV spectrometer. The solid circles in Fig. 4(b) show the divergence of the 61st harmonic at the gas jet positions around $z = -18$ mm. The lowest divergence of the 61st harmonic was 0.5 mrad at $z = -18$ mm, due to the realization of the flattened laser profile that allows a large harmonic generation cross section. Since the 61st harmonic had its maximum efficiency and minimum divergence at $z = -18$ mm, the brightness of the 61st harmonic was greatly increased, as shown by the solid squares in Fig. 4(b). The harmonic brightness here is defined as the power of a harmonic per unit area per unit solid angle subtended at the source. We estimated the harmonic pulse duration of 8 fs from the spectral width and the source radius of 70 μm. At $z = -18$ mm, the brightness of the 61st harmonic was estimated to be over 1×10^{15} W/cm^2/srad (also a conservative value). Thus, we have accomplished bright high-order harmonic generation by exploiting the profile-flattened and self-guided laser pulses interacting with the long gas jet medium.

A further analysis on the spectral structure of high-order harmonics was performed by controlling the initial laser chirp. It

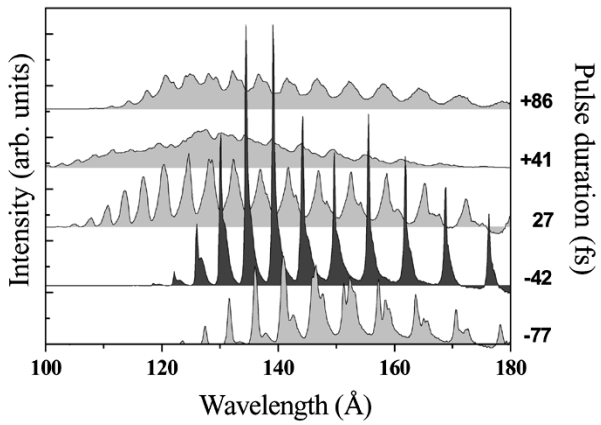

Fig. 5. Harmonic spectra from Ne driven by femtosecond laser pulses with different laser chirp at the gas jet pisition of $z = -18$ mm. Sign of the pulse duration refers to the sign of applied laser chirp.

is well known that high-order harmonics can have dynamically induced negative chirp, which originates from the temporal variation of the harmonic phase that is dependent on laser intensity. In addition, the laser pulses can acquire a positive chirp in the leading edge due to SPM in an ionizing medium, as discussed in Section II. Since high-order harmonics are coherently generated through the interaction of atoms with the laser pulse, the laser chirp induced by SPM is transferred to the harmonic chirp. When the harmonics are mainly generated in the leading edge, two different harmonic chirps, i.e., dynamically induced negative chirp and SPM-induced positive chirp, can compete and affect the spectral structure of high-order harmonics. Since chirped laser pulses can either compensate or enhance the harmonic chirp, the spectral structure of harmonics can be controlled by applying appropriately chirped laser pulses.

Fig. 5 shows the chirp dependence of harmonic spectra for the Ne gas jet placed at $z = -18$ mm. Even though the harmonic generation was maximized at this gas jet position, the harmonic spectrum can be broadened due to the chirp of the harmonics. The laser chirp was controlled by changing the grating separation in the pulse compressor while keeping the laser energy fixed. The negative chirp of the 42-fs pulse generated the sharpest and brightest harmonics due to the realization of chirp compensation. As seen in Fig. 3, the negatively chirped 42-fs pulse was transformed into a positive chirp in the leading edge of the laser pulse during the propagation through the ionizing 9-mm Ne medium. Since phase-matched harmonics were generated mainly in the leading edge, this positive chirp provided a suitable condition for compensating the dynamically induced negative harmonic chirp, resulting in the generation of sharp and bright high-order harmonics. With the negatively chirped 42-fs pulse, the bandwidth of the 61st harmonic was obtained to be 0.07 nm and the spectral brightness was enhanced four times over that obtained from a chirp-free 27-fs pulse. On the other hand, the positively chirped 41-fs pulse, which enhanced the harmonic chirp, produced a quasi-continuous harmonic spectrum. The quasi-continuous harmonics can be useful for such applications as the ultrafast X-ray absorption spectroscopy that

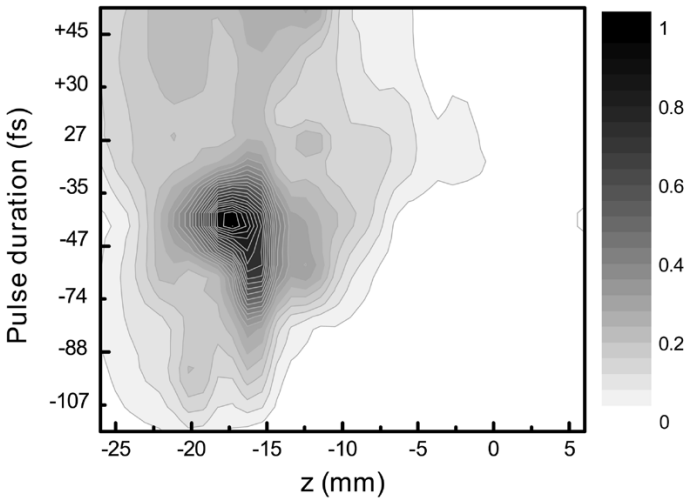

Fig. 6. Spectral brightness of 61st harmonic with respect to gas jet position and laser chirp.

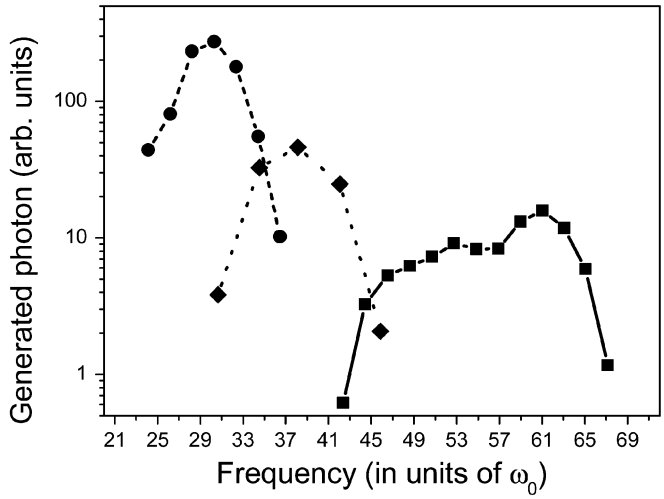

Fig. 7. Relative harmonic yield with respect to harmonic order from three cases. Solid squares are for harmonics from a 9-mm Ne gas jet and solid circles from a 6-mm Ar gas jet at the self-guiding conditions. Diamonds indicate harmonics from He driven by a two color field.

requires broadband X-rays in a femtosecond duration. This laser chirp control is quite simple in a CPA laser and, thus, will be a valuable technique to control the spectral structure of harmonics depending on the applications.

The laser propagation, especially for profile flattening and self-guiding, did not depend sensitively on the laser chirp. We examined the spatial profile changes with respect to the laser chirp sign by 3-D simulation. In the simulation, the sign of the chirp did not influence the profile flattening because the ionization level created by pulses with different chirp, but with same field intensity, is essentially the same. In the case of a chirp-free 27-fs pulse, the self-guiding and profile flattening was observed at a slightly different laser intensity and the radius of the waveguiding region was also slightly changed. With 27-fs pulses, the laser intensity and radius in the flattened area were increased by 11% and 13%, respectively, compared to those for 42-fs pulses. The difference in the harmonic spectra between the cases of the positively chirped 41-fs and negatively chirped 42-fs pulses occurs mainly due to the different amounts of harmonic chirp. Therefore, the spectral structure of harmonics can be controlled by using chirped laser pulses without disturbing the self-guided propagation much.

Since the high-order harmonic generation can be controlled by adjusting the gas jet position and laser chirp, an optimized condition of harmonic generation can be found by varying the gas jet position and laser chirp. Fig. 6 shows the spectral brightness of the 61st harmonic with respect to gas jet position and laser chirp. It clearly shows that the maximum spectral brightness of the 61st harmonic with the gas jet position occurs at about $z = -18$ mm and for a negatively chirped 42-fs laser pulse. Thus, the optimization of harmonic brightness in the space and time domains was achieved by appropriately selecting the gas jet position and laser chirp.

We extended bright harmonic generation using different noble gases. Fig. 7 shows the relative harmonic yield from thee different species, i.e., He, Ne, and Ar, with respect to harmonic order. The squares show the harmonic yield from a 9-mm Ne gas jet obtained using the self-guiding and laser chirp control techniques. The circles in Fig. 7 show the optimized harmonics from a 6-mm Ar gas jet [10] by selecting a proper gas jet position, which also resulted in a self-guided laser propagation. The harmonics are optimized at the gas jet position of $z = -7$ mm and the energy of the optimized 29th harmonic was about 4 nJ with a single laser shot of 5 mJ. The diamonds represent harmonics from a 6-mm He gas jet driven by the two-color laser field comprising of an 820-nm laser field and its second harmonic [22]. Harmonics from He are normally weaker than those from Ne due to the smaller atomic response of He. However, we obtained bright harmonic generation from He using the simple method of inserting a second harmonic crystal between a focusing mirror and an He gas jet. In this case, we selected a gas jet position $z = -10$ mm for proper laser propagation. The efficiency of conversion to second harmonic was over 18%, which created an intense second harmonic field for the interaction. In the experiment, bright harmonics were generated at every fourth order from the 30th harmonic and the brightest harmonic was the 38th. The energy of the 38th harmonic exceeded 2 nJ with 2-mJ fundamental laser pulse and its second harmonic. Consequently, we produced bright harmonics from He, Ne, and Ar that covered the wavelength region from 30 to 13 nm.

IV. Interferometry With High-Order Harmonics

Since high-order harmonics are generated by the coherent interactions between atoms and a laser field, the coherence property of the laser field can be inherited by the harmonics. We performed interferometry experiments with a spatially divided pair of harmonic beams and with two temporally separated harmonic pulses. Previously, we reported the measurement of spatial coherence of harmonics from Ar using a double-pinhole interference [2]. A perfect coherence was observed

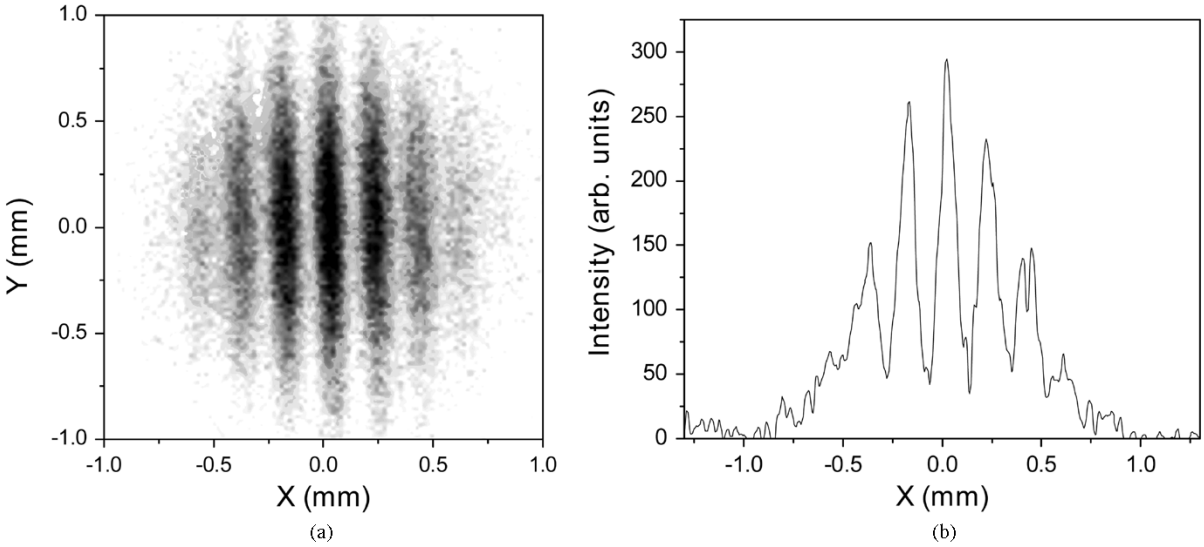

Fig. 8. Double-pinhole interferogram of bright harmonics from a 9-mm Ne gas jet with 60-μm pinhole separation: (a) fringe pattern and (b) horizontal intensity profile of the interferogram.

in most of the beam cross sections with harmonics from Ar that were controlled to have a narrow spectral width. The spatial coherence of harmonics from a 9-mm Ne gas jet was also examined by observing the double-pinhole interference. In addition, we examined the spectral interference by two temporally separated harmonic pulses from a 6-mm Ar gas jet. The spectral interference between two high-order harmonic pulses was obtained using temporally phase-locked harmonic sources generated from two intense laser pulses with a time delay [15]. These two types of interference measurements demonstrate that the harmonics are phase locked in time and space.

At first, the spatial coherence of bright harmonics from 9-mm Ne gas jet was investigated with double-pinhole interference. The harmonics were generated by using negatively chirped 48-fs laser pulses at the optimized conditions for the 61st harmonic as indicated in Fig. 6. A thick Al foil (18- μm thickness) with two pinholes was placed 25 cm after the gas medium. Each pinhole had a 10-μm diameter, and the separation between them was 60 μm. The harmonic beam size was about 100 μm on the double-pinhole plate. Fig. 8 shows the interference pattern recorded on an X-ray CCD located 80 cm from the double-pinhole plate and its horizontal intensity profile. The fringe visibility was 0.7 at the center of interference pattern. Even though the bright harmonics from a 9-mm Ne gas jet did not exhibit full spatial coherence due to the broad spectrum from 12 to 20 nm, it still had a quite good coherence. With two pinholes with 100-μm separation, we observed a fringe visibility of 0.5. Thus, the bright harmonics from the 9-mm Ne gas jet possessed a good spatial coherence.

Next, we obtained the spectral interference between high-order harmonics driven by two temporally separated laser pulses. We performed the experiment using a 6-mm Ar gas jet and two identical chirp-free 25-fs laser pulses of 1-mJ energy. The peak gas density was about 60 torr. The temporally separated pair of laser pulses was prepared using a Michelson interferometer setup and the time delay between the pulses was controlled by a piezoelectric translator. When the gas jet was placed 10 mm before the laser focus, the harmonics were bright enough to measure the spectral interference with a single laser shot. Fig. 9 shows the spectral interference of the harmonics from the 21st to the 27th generated by the two laser pulses with 52-fs time delay. The spectral interference was clearly observed and the fringe visibility was about 0.7 for the 23rd harmonic. A previous result, reported by Salieres *et al.* [15], showed a similar visibility for the 15th harmonic, but very low visibility for the 23rd harmonic. Our results show that the two temporally separated laser pulses can generate two temporally phase-locked harmonics up to the 27th order.

In addition, we observed spectral interference even though the two laser pulses were significantly overlapped in time. The spectral interference patterns of the 23rd harmonic with time delays of 52-fs (dotted line) and 23-fs (solid line) are shown in Fig. 10(a). One interesting result was that the fringe pattern was observed with the time delay shorter than the pulse duration. Usually, temporally overlapped pulses cannot form the spectral interference. However, an intensity dip in the middle of the two laser pulses, which is created by the destructive interference between two temporally overlapped pulses, can generate an interference pattern due to the nonlinearity of harmonic generation. We performed strong field approximation (SFA) simulations [23], combined with a coherent sum method [24], to obtain the spectral interference of harmonics in the case of overlapped laser pulses. The solid line in Fig. 10(b) shows the clear interference pattern with 23.2-fs time delay, which induces a destructive interference in the middle of the two laser pulses. However, with a slightly longer time delay of 24.5 fs, the fringe pattern disappears due to a constructive interference of the two pulses in the overlapped part. This result shows that we can generate temporally phase-locked harmonic

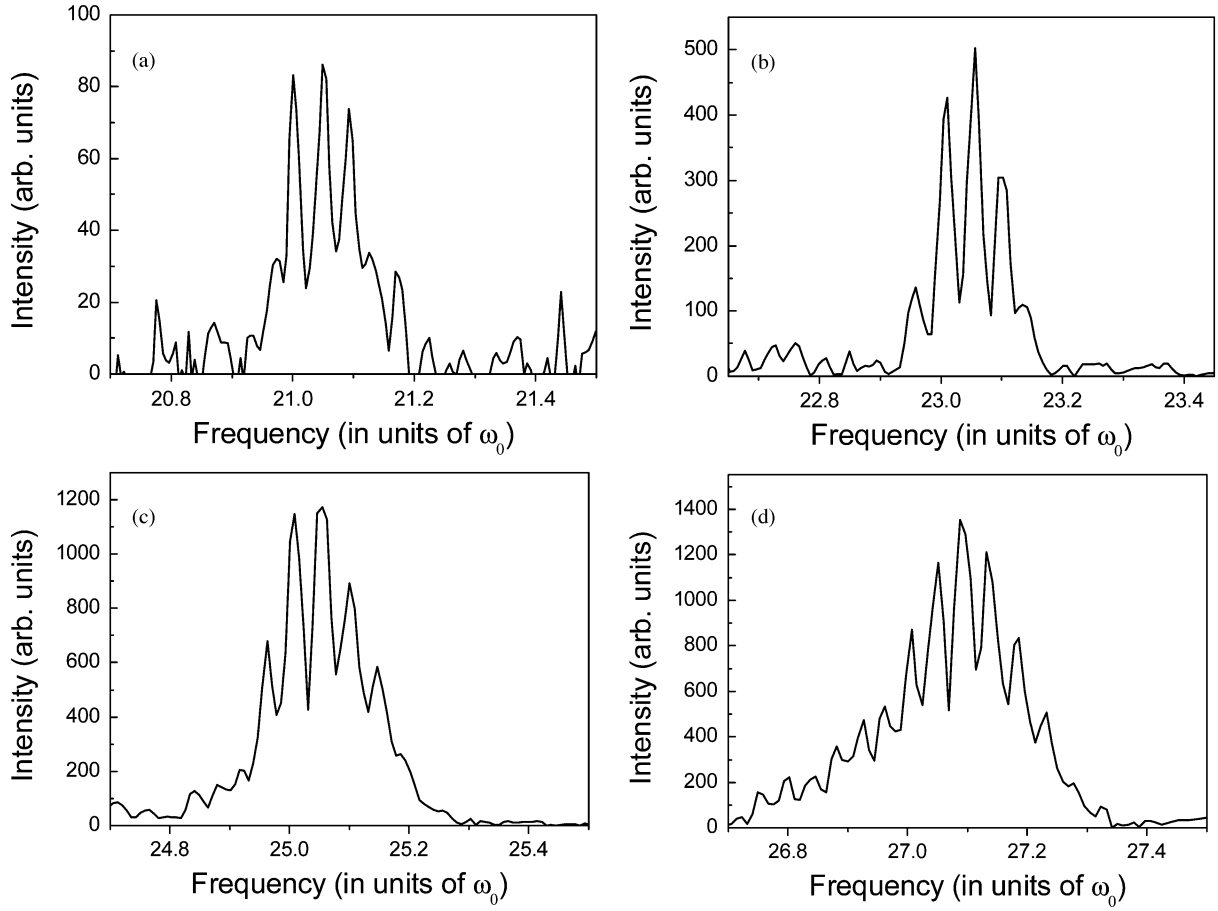

Fig. 9. Spectral interference of harmonics from a 6-mm Ar gas jet driven by two laser pulses with 52-fs time delay: (a) 21st, (b) 23rd, (c) 25th, and (d) 27th harmonics.

pulses with a time delay shorter than the pulse duration of the driving laser field by selecting the proper phase relation between two laser fields.

In this section, we have presented the details of two kinds of interference properties of harmonics: one was double-pinhole interference for the investigation of spatial coherence, and the other was the spectral interference formed by a pair of temporally phase-locked harmonic pulses. Since the coherence properties of harmonics are important for applications to EUV interferometry, holography, plasma diagnostics, and metrology, the investigation of the coherence properties of harmonics will be valuable for future applications of harmonic EUV/soft X-ray sources.

V. Conclusion

We have presented methods to generate bright harmonics from long gas jets in a wide spectral range. First, we investigated the profile flattening and self-guiding conditions, which are essential to generate bright harmonics from a long and high-density medium. For the cases of Ar and Ne, we enhanced the harmonic generation efficiency by using profile-flattened and self-guided laser pulses. By the combination of self-guiding and laser chirp control, we generated bright 61st harmonic at 13 nm from a 9-mm Ne gas jet with narrow spectral bandwidth. Since high-reflectivity Mo:Si mirrors are available at this wavelength, this method can be applied for the harmonic source development for EUV metrology. For He, we obtained very strong harmonics from a 6-mm He gas jet in a two-color laser field.

We then measured the interference patterns of harmonic beams to examine the coherence properties of the bright harmonics from long gas jets. We tested the spatial coherence of harmonics from Ne using a double-pinhole interference. It showed a good spatial coherence of harmonics in most of the beam cross section. The spectral interference between a temporally phase-locked pair of harmonic pulses was also observed by using temporally separated laser pulses. These two types of interferometry indicate that the high-order harmonics can be applied to various spatial and temporal measurements with good coherence. In brief, we have demonstrated methods to generate bright high-order harmonics with good coherence properties in space and time.

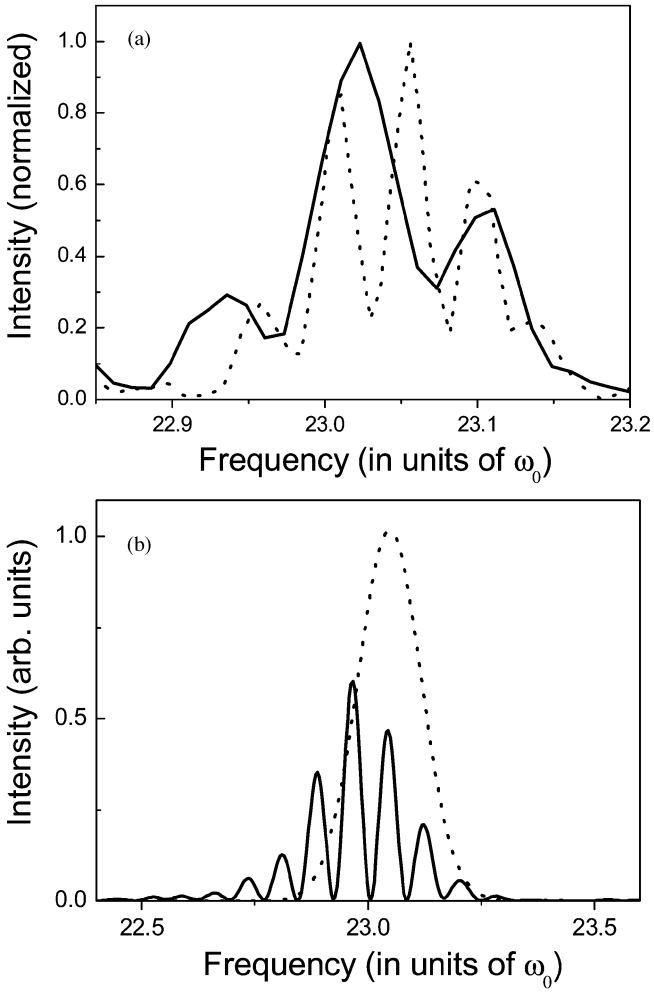

Fig. 10. (a) Spectral interference of the 23rd harmonic driven by two laser pulses of 52-fs (dotted line) and 23-fs (solid line) time delays. (d) Spectral interference of 23rd harmonic calculated using a SFA model with two laser pulses of 23.2-fs (dotted line) and 24.5-fs (solid line) time delays.

REFERENCES

[1] R. A. Bartels, A. Paul, H. Green, H. C. Kapteyn, M. M. Murnane, S. Backus, I. P. Christov, Y. Liu, D. Attwood, and C. Jacobson, "Generation of spatially coherent light at extreme ultraviolet wavelengths," *Science*, vol. 297, pp. 376–378, 2002.

[2] D. G. Lee, J. J. Park, J. H. Sung, and C. H. Nam, "Wave-front measurements of high-order harmonic beams by use of point-diffraction interferometry," *Opt. Lett.*, vol. 28, pp. 480–482, 2003.

[3] H. T. Kim, D. G. Lee, K.-H. Hong, J.-H. Kim, I. W. Choi, and C. H. Nam, "Continuously tunable high-order harmonics from atoms in an intense femtosecond laser field," *Phys. Rev. A*, vol. 67, no. 051 801 (R), 2003.

[4] Y. Mairesse, A. de Bohan, L. J. Frasinski, H. Merdji, L. C. Dinu, P. Monchicourt, P. Breger, M. Kovačev, R. Taïeb, B. Carré, H. G. Muller, P. Agostini, and P. Salières, "Attosecond synchronization of high-harmonic soft X-rays," *Science*, vol. 302, pp. 1540–1543, 2003.

[5] C. Spielmann, N. H. Burnett, S. Sartania, R. Koppitsch, M. Schnürer, C. Kan, M. Lenzner, P. Wobrauschek, and F. Krausz, "Generation of coherent X-rays in the water window using 5-femtosecond laser pulses," *Science*, vol. 278, pp. 661–664, 1997.

[6] M. Schnürer, Z. Cheng, M. Hentschel, G. Tempea, P. Kálmán, T. Brabec, and F. Krausz, "Absorption-limited generation of coherent ultrashort soft-X-ray pulses," *Phys. Rev. Lett.*, vol. 83, pp. 722–725, 1999.

[7] A. Baltuška, Th. Udem, M. Uiberacker, M. Hentschel, E. Goulielmakis, Ch. Gohle, R. Holzwarth, V. S. Yakovlev, A. Scrinzi, T. W. Hänsch, and F. Krausz, "Attosecond control of electronic processes by intense light fields," *Nature*, vol. 421, pp. 611–615, 2003.

[8] E. Constant, D. Garzella, P. Breger, E. Mével, Ch. Dorrer, C. Le Blanc, F. Salin, and P. Agostini, "Optimizing high harmonic generation in absorbing gases: Model and experiment," *Phys. Rev. Lett.*, vol. 82, pp. 1668–1671, 1999.

[9] S. Kazamias, D. Douillet, F. Weihe, C. Valentin, A. Rousse, S. Sebban, G. Grillon, F. Augé, D. Hulin, and Ph. Balcou, "Global optimization of high harmonic generation," *Phys. Rev. Lett.*, vol. 90, no. 193 901, 2003.

[10] D. G. Lee, H. T. Kim, K.-H. Hong, and C. H. Nam, "Generation of bright low-divergence high-order harmonics in a long gas jet," *Appl. Phys. Lett.*, vol. 81, pp. 3726–3728, 2002.

[11] V. Tosa, E. Takahashi, Y. Nabekawa, and K. Midorikawa, "Generation of high-order harmonics in a self-guided beam," *Phys. Rev A*, vol. 67, no. 063 817, 2003.

[12] H. T. Kim, I. J. Kim, D. G. Lee, K.-H. Hong, Y. S. Lee, V. Tosa, and C. H. Nam, "Optimization of high-order harmonic brightness in the space and time domains," *Phys. Rev. A*, vol. 69, no. 031 805(R), 2004.

[13] D. G. Lee, J.-H. Kim, K.-H. Hong, and C. H. Nam, "Coherent control of high-order harmonics with chirped femtosecond laser pulses," *Phys. Rev. Lett.*, vol. 87, no. 243 902, 2001.

[14] H. T. Kim, I. J. Kim, K.-H. Hong, D. G. Lee, J.-H. Kim, and C. H. Nam, "Chirp analysis of high-order harmonics from atoms driven by intense femtosecond laser pulses," *J. Phys. B: At. Mol. Opt. Phys.*, vol. 37, pp. 1141–1152, 2004.

[15] P. Salières, L. Le Déroff, T. Auguste, P. Monot, P. d'Oliveira, D. Campo, J.-F. Hergott, H. Merdji, and B. Carré, "Frequency -domain interferometry in the XUV with high-order harmonics," *Phys. Rev. Lett.*, vol. 83, pp. 5483–5486, 1999.

[16] M. Bellini, C. Corsi, and M. C. Gambino, "Neutral depletion and beam defocusing in harmonic generation from strongly ionized media," *Phys. Rev. A*, vol. 64, no. 023 411, 2001.

[17] J.-H. Kim and C. H. Nam, "Plasma-induced frequency chirp of intense femtosecond lasers and its role in shaping high-order harmonic spectral lines," *Phys. Rev. A*, vol. 65, no. 033 801, 2002.

[18] C. H. Cha, Y. I. Kang, and C. H. Nam, "Generation of a broad amplified spectrum in a femtosecond terawatt Ti:Sapphire laser using a long wavelength injection method," *J. Opt. Soc. Amer. B*, vol. 16, pp. 1220–1223, 1999.

[19] L. Cohen, "Time-frequency distributions—A review," *Proc. IEEE*, vol. 77, pp. 941–981, 1989.

[20] J.-H. Kim, D. G. Lee, H. J. Shin, and C. H. Nam, "Wigner time-frequency distribution of high-order harmonics," *Phys. Rev. A*, vol. 63, no. 063 403, 2001.

[21] I. W. Choi, J. U. Lee, and C. H. Nam, "Space-resolving lat-field XUV spectrograph system and its aberration analysis with wave front aberration," *Appl. Opt.*, vol. 36, pp. 1457–1466, 1997.

[22] I. J. Kim, H. T. Kim, C. M. Kim, J. J. Park, Y. S. Lee, K. H. Hong, and C. H. Nam, "Efficient high-order harmonic generation in a two-color laser field," *Appl. Phys. B*, vol. 78, pp. 859–861, 2004.

[23] M. Lewenstein, Ph. Balcou, M. Yu Ivanov, A. L'Huillier, and P. B. Corkum, "Theory of high-harmonic generation by low-frequency laser fields," *Phys. Rev. A*, vol. 49, pp. 2117–2132, 1994.

[24] J. H. Kim, H. J. Shin, D. G. Lee, and C. H. Nam, "Enhanced spectral resolution of high-order harmonics by the coherent sum of dipole spectra," *Phys. Rev. A*, vol. 62, no. 055 402, 2000.

[25] H. J. Shin, D. G. Lee, K.-H. Hong, and C. H. Nam, "Generation of nonadiabatic blueshift of high harmonics in an intense femtosecond laser field," *Phys. Rev. Lett.*, vol. 83, pp. 2544–2547, 1999.

H. T. Kim received the Ph.D. degree in physics from the Korea Advanced Institute of Science and Technology (KAIST), Daejeon, in 2004.

He is a Postdoctoral Researcher at the same institute. His current research interests include ionization effects on femtosecond laser pulse propagation and high-order harmonic generation from molecules.

I. J. Kim is currently working toward the Ph.D. degree in physics from the Korea Advanced Institute of Science and Technology (KAIST), Daejeon.

His current research interests include high-order harmonic generation driven by two-color laser fields.

V. Tosa was born in Bedeciu, Romania, in 1955. He received the B.S. degree in physics (with a thesis on energy band calculations) and the Ph.D. degree for work done on multiphoton excitation and vibration relaxation of polyatomic molecules, from "Babes-Bolyai" University Cluj-Napoca, Romania, in 1979 and 1992, respectively.

Since 1982, he has been a Researcher at the National Institute for Research and Development in Isotopic and Molecular Technologies, Cluj-Napoca, where he is currently a Principal Investigator. His research interests include computer modeling of laser interaction with atoms and molecules (multiphoton processes, high-order harmonic generation). He also works in computer modeling of substance migration in multilayer packaging systems.

Dr. Tosa is a member of the Romanian Physical Society and SPIE.

C. M. Kim is working toward the Ph.D. degree in physics from the Korea Advanced Institute of Science and Technology (KAIST), Daejeon.

His current research interests include theoretical understanding and computer simulation of high-order harmonic generation.

J. J. Park is working toward the Ph.D. degree in physics from the Korea Advanced Institute of Science and Technology (KAIST), Daejeon.

His current research interests include XUV holography using high-order harmonics.

Y. S. Lee is working toward the Ph.D. degree in physics from the Korea Advanced Institute of Science and Technology (KAIST), Daejeon.

His current research interests include CEP stabilization of laser pulses emitted by a kilohertz CPA system.

A. Bartnik, photograph and biography not available at the time of publication.

H. Fiedorowicz, photograph and biography not available at the time of publication.

C. H. Nam received the B.S. degree in nuclear engineering from Seoul National University, Seoul, Korea, the M.S. degree in physics from the Korea Advanced Institute of Science and Technology (KAIST), Daejeon, and the Ph.D. degree in plasma physics from Princeton University, Princeton, NJ.

He has been a Professor at KAIST since 1989.